Multi-band optical/IR transmissometry during the VAMPIRA trials, spring 2004

Arie N. de Jong, Leo H. Cohen, Marcel M. Moerman
TNO - Physics and Electronics Laboratory, The Hague – Netherlands

ABSTRACT

Scattering by atmospheric aerosols is one of the environmental parameters determining the range performance of optical and infrared sensors. Extinction of the target contrast along the path due to scattering is difficult to estimate in real operational conditions due to uncertainties in the size distribution of the particles, their constitution and concentration along the path. Knowledge on their behaviour allows calculation of the atmospheric transmission by means of standard scattering formulae. In-situ measurement of the characteristics of the particles by means of counters provides data of limited value due to the possible impact of the direct environment. The data may also be not representative for the particles at other locations along the path. Similarly the measurement of the particle characteristics by means of LIDAR provide an asymmetric view, while the backscatter by the particles is difficult to translate into extinction coefficients in forward direction. Multi-band transmissometry along the path of interest provides however direct information on the real atmospheric propagation characteristics. Furthermore the multi-band data allow the validation of the aerosol model, to be used in transmission models such as MODTRAN. The VAMPIRA trials, organised in March/April 2004 by Germany in the Baltic Sea near Eckernförde, provided an opportunity to test the usefulness of a 7-channel optical/IR transmissometer, developed at TNO-FEL. In this paper the set-up of the system is described and samples of data are presented. The multi-band transmission data, collected over an 8.6 km path over water, are compared with extinction values obtained from in-situ particle measurements. The data show clearly that the aerosols have rural characteristics during most of the time.

Keywords: atmospheric transmission, aerosols, optical/IR transmissometer, multi-band

1. INTRODUCTION

Atmospheric transmission characteristics are directly responsible for the range performance of optical and infrared sensors [1]. The major physical effects in the propagation process are: molecular absorption, local variations of the refractive index of the air, their fluctuations in time and scattering by aerosols [2]. As a consequence the target contrast is decreased, ray bending and blurring occur due to atmospheric refraction while turbulence (the local temporal variations of the refractive index of air) effects result in scintillation and beam wander. Scintillation implies rapid fluctuations of the radiant intensity contrast of a point-like target, while beam wander implies rapid fluctuation of the apparent direction of the target. In the meantime the presence of particles (aerosols) in the air leads to scattering: on the one hand target radiation is scattered away from the line of sight (LOS), on the other hand terrestrial or sky radiation may be scattered into the LOS. The radiation scattered away implies a direct loss in target contrast; the radiation scattered into the LOS may lead to contrast loss for optical sensors, where contrast is defined as the ratio of the radiance difference between target and background and the average background radiance.

Various atmospheric propagation experiments have been carried out during the last decade for validation of transmission models such as MODTRAN [3]. For practical reasons and for reasons of operational interest (littoral warfare), most of these experiments have been carried out in a coastal zone such as EOPACE [4] and POLLEX [5]. During these experiments, all physical phenomena mentioned before, were investigated. One of the lessons learned was that proper quantitative understanding of the measured effects was difficult due to the lack of data on the meteorological parameters and their vertical profile along the path. For example the vertical profile of the air temperature, being responsible for refractive transmission gain, is hard to measure directly. It was shown, that the measurement of atmospheric distortion from a lamp array at long distance provides a profile, which can be used in the gain model [6]. Variation of the temperature profile along the path will result in typical transmission effects [7]. It was also shown, that scintillation,

Optics in Atmospheric Propagation and Adaptive Systems VII,
edited by John D. Gonglewski, Karin Stein, Proceedings of SPIE Vol. 5572
(SPIE, Bellingham, WA, 2004) · 0277-786X/04/$15 · doi: 10.1117/12.581278

measured at overseas paths, did not correspond to local coastal turbulence measurements [8]. An important contribution to the magnitude of scintillation appears to be caused by mid-path waves at the water surface, tilting the profile [9].

Similarly uncertainties are introduced in optical and IR atmospheric propagation by aerosols. Prediction of their scattering characteristics requires knowledge on the composition, the size distribution and concentration. Furthermore these properties may vary along the path, especially in coastal locations [10]. Another source of complexity is the change in properties with time, determined by the wind speed and direction as well locally as on mesa scale. The origin of the particles may be maritime or continental, with components from urban or industrial activities. As a consequence discrepancies can easily arise when a path integrated transmission measurement is compared with predictions from local particle measurements. A typical example of such a discrepancy is shown in Figure 1, taken from one of the EOPACE experiments in San Diego (31 August 1997). Particle size and concentration measurements are converted to extinction coefficients and path transmissions as if the particle characteristics were the same over the whole path. The really measured transmission is only slightly reduced while the prediction due to aerosols shows a very strong reduction in transmission between 06.00 to 09.00 (UTC).

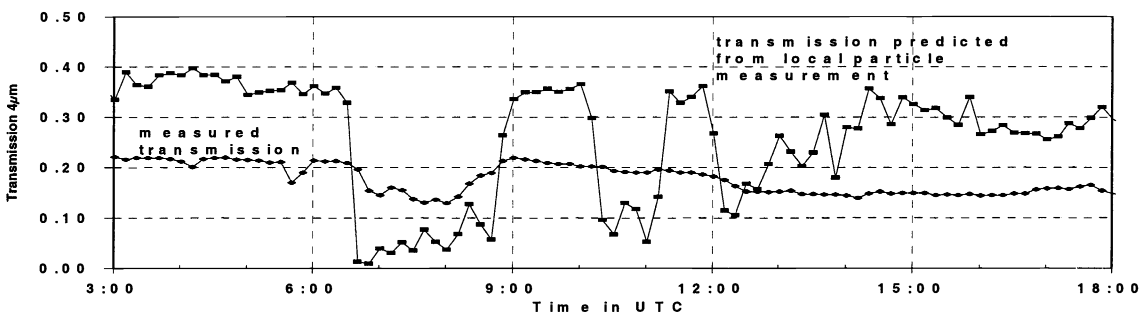

Figure 1. Example of discrepancy between measured and predicted transmission on 31 August 1997 over 15 km path San Diego Bay due to variation in particle concentration along the path; T(air)=20°C, T(sea)=22°C, RH=85%, wind speed: 1m/s, direction: West, all measured at mid-path buoy; particles measured at IB pier

This kind of results has been found frequently and culminates in the case of local showers. During some experiments particle counters were installed on a boat in order to investigate variations of the particle concentration along the path, while a calibrated source was mounted on the boat, acting as one side of a transmissometer link. Here problems were found due to the influence of the boat on the particle characteristics. A multi-band transmissometer for investigating the characteristics of battlefield obscurants has been used before [11]. Transmission values in optical and IR bands relate directly to extinction coefficients and associated particle size distribution. The same idea was successfully tested during the last EOPACE experiments in Duck (NC), where it was shown that the aerosols were of maritime nature [12]. The VAMPIRA trials, organised by the German Ministry of Defence in the Baltic Sea March/April 2004, provided another opportunity to test the usefulness of this idea due to the favourable range of 8.6 km with easy access at both sides. TNO-FEL thus installed their 7-channel optical/IR transmissometer over the Eckernförde Bucht simultaneously with particle counters on one side and meteorological equipment on both sides and on a mid-path buoy.

2. MODEL CONSIDERATIONS

It is well known that scattering of electromagnetic waves by a particle depends on the size of the particle, the (complex) refractive index of its material and the wavelength of the electromagnetic wave. Two scattering characteristics are of prime interest: the extinction cross section C_{ext} and the scatter diagram or phase function. The extinction cross section reaches an asymptotical limit of 2x the geometrical cross section for particles having a diameter of more than three times the wavelength. The scatter diagram (the radiation per steradian in a given direction) is generally broad (60°) for particles with the same size as the wavelength, similar to the diffraction pattern of a circular aperture. For a cloud of particles, each having a different size, the size distribution plays an important role. Recent studies have provided an enhanced knowledge on particle size distributions at sea thanks to the MAPTIP, EOPACE and LAPTEX experiments [13, 14, 15, 16, 17]. The knowledge concerns especially the bigger particles close to the sea surface, as created by breaking waves in the surf zone.

The standard MODTRAN model can handle a number of particle size distributions such as the classical Navy Aerosol Model (NAM) and the Rural model. When using the MODTRAN code, one can import the visibility as parameter. In order to illustrate the impact of using the NAM and Rural aerosol models, the dependence of the extinction coefficient on the wavelength is shown for two visibilities for both cases in Figure 2. The NAM models implies clearly less dependence of the scattering cross section with wavelength. Figure 3 similarly shows the transmission over an 8.6 km path for both models and different visibilities. The Log T(λ_1) versus Log T(λ_2) plots show different slopes in both cases, those of the NAM model being steeper for the bands chosen. This effect stimulates the use of a multi-band transmissometer for investigating the real type of aerosol, present during the campaign.

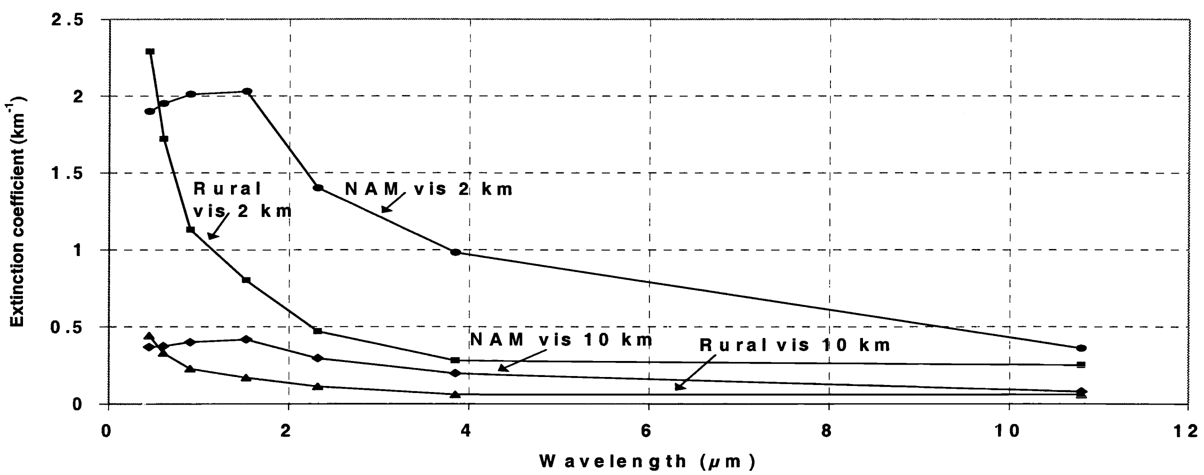

Figure 2. Dependence of the aerosol extinction coefficient of the wavelength for NAM and Rural aerosol model according to MODTRAN transmission model

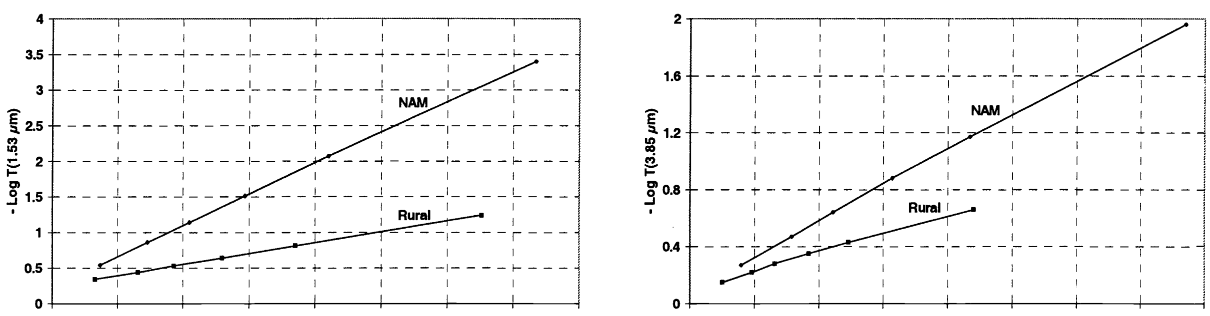

Figure 3. [10]Log plots of the transmission T in one spectral band versus the transmission in another spectral band as predicted by MODTRAN, using the NAM or Rural aerosol model; the path-length is 8.6 km, T(air)=5 °C, RH=80%, the visibility varies from 40 (right) to 4 km (left).

3. SITE DESCRIPTION

One of the objectives of the VAMPIRA trial was the demonstration of the synergy between radar and IR sensors in a littoral maritime environment. For this reason a trials location and season was selected with a high probability of occurrence of a positive Air - Sea Temperature Difference (ASTD). This was found to be in the southern Baltic Sea at the German "Erprobungsstelle" WTD 71 at Sürendorf near Eckernförde. A sketch of the local situation is shown in Figure 4.

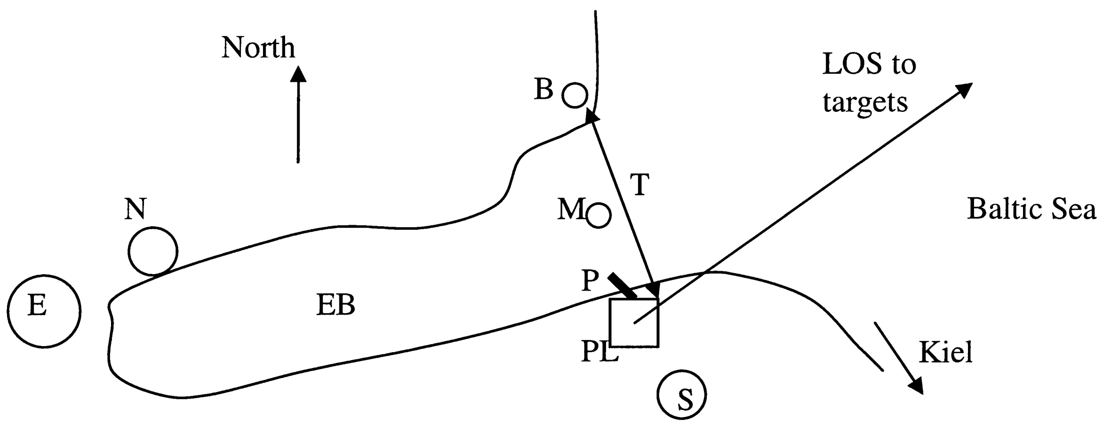

Figure 4. Schematic drawing of the VAMPIRA trials location. E = Eckernförde, S = Sürendorf, B = Booknis Eck, EB = Eckernförde Bucht, P = Pier at WTD 71, PL = platform with radar and IR sensors, T = transmission path of TNO-FEL with 8.6 km length, M = location of TNO buoy, N = German Naval Base

At the main trials location at WTD 71 sensors were located on an elevated platform. Data were taken with these sensors of point targets, mounted on a boat or helicopter, making inbound and outbound runs at various times of the day. Another activity at WTD 71 took place at the pier, at which extensive meteorological equipment was installed, including sensors for characterizing atmospheric particles, such as two PMS probes and an integrating nephelometer from TNO-FEL. At Booknis Eck, on the opposite side of the bay, the optical/IR receiver and the radar transmitter were installed by TNO-FEL for the two transmission links. The radar receiver was located at the end of the pier, while the optical-IR source was located at the beginning of the pier near the coastline. In addition a transmission link was installed by SPAWAR in the opposite direction: the source at Booknis Eck and the receiver at the end of the pier. FGAN installed a high resolution and high frame rate optical camera system between Booknis Eck and the beginning of the pier for measurement of atmospheric blur and scintillation. TNO-FEL installed a meteo buoy with T and RH sensors at 5 heights at a mid-path location between Booknis Eck and WTD 71. TNO also installed met stations at the pier and at Booknis Eck. The average water depth along the transmission path is about 20 m.

4. DESCRIPTION OF EQUIPMENT

Most of the equipment from TNO-FEL, used during VAMPIRA, is of standard use and will therefore not be described here. In this section attention will be spent on the multi band transmissometer MSRT, as developed at TNO-FEL [18]. The source of the system is actually a double source to cover the complete optical/IR spectral band from 0.4 – 14 μm. One of the sources uses a standard tungsten lamp (50 or 100 Watt), located in the focal plane of an off-axis parabolic reflector with 300 mm focal length. The other source uses similarly an electrically heated ceramic bar. Both sources are mounted in one housing and use the same mechanical chopper, which modulates the light with a fixed frequency, in this case 1160 Hz. A pick-up signal for reference purposes is sent to a BNC output connector for further transmission by means of a radio-link to the receiver side (radio frequency: 400.200 MHz). The entrances are covered with plastic window material with appropriate transmittance in the various spectral bands. For wavelengths between 1.5 and 4 μm both sources contribute to the signal output. The beam divergence of the sources is about 4.5x15 mrad for the visual source and 6x50 mrad for the IR source.

Table 1. Summary of the main characteristics of the MSRT transmissometer

Channel No	Spectral band (μm)	Focal length (mm)	FOV (mrad)	Pupil size (mm)	Reduced pupil (mm)	Source RIC (W/sr)	Gain	100% DC signal (V) at 8.6 km	S/N ratio @ 1.1 s int. time
1	0.40-0.49	35	73	35	20x20	290	1000	1.00	90
2	0.57-0.65	35	77	50	10x10	1020	100	0.47	1800
3	0.78-1.04	35	77	35	10x10	4600	100	2.23	13200
4	1.39-1.67	35	86	50/30	10x10	6500	100	2.96	1300
5	2.12-2.52	12	83	18	10x10	950	100	0.134	390
6	3.55-4.15	125	16	55	same	55	100	5.51	5700
7	7.8-13.7	75	27	75	same	42	1000	0.45	82

At the receiver side the signals are collected by means of the seven pupils of the multi-band radiometer. The main characteristics of the MSRT receiver are shown in Table 1. The detector material for channels 1-3 is Silicon; for channels 4 and 5 InGaAs detectors are used, while channels 6 and 7 use Liquid Nitrogen cooled InSb respectively HgCdTe detectors. During the VAMPIRA trials reduced pupil sizes had to be applied due to the fact that during the morning and early afternoon too much scattered sunlight entered the sensor pupils. This is due to the large Field of Views (FOV) of each of the visual/Near IR channels. This FOV is chosen due to the main purpose of the transmissometer as smoke and obscurants characterization system in multiple Lines of Sight (LOS). The gain can be set in the pre-amplifiers by means of a gain control system, installed as software in an associated PC. The amplified signals are sent to a set of seven Lock-In amplifiers. By using the reference signal, received through the radio link, seven DC outputs are created recorded on a multi-band data logger with 16 bits dynamic range. The integration times have been set to 1.1 second. The data of the seven channels are sampled with a frequency of 5 Hz. The system was calibrated before and after the VAMPIRA trial in the dark tunnel at TNO-FEL with a distance between source and receiver of 60 m. In this procedure, the pupils of the sources were limited in size in order to avoid saturation. Pictures of the source and the receiver as well as the container in Booknis Eck are shown in Figures 5 and 6.

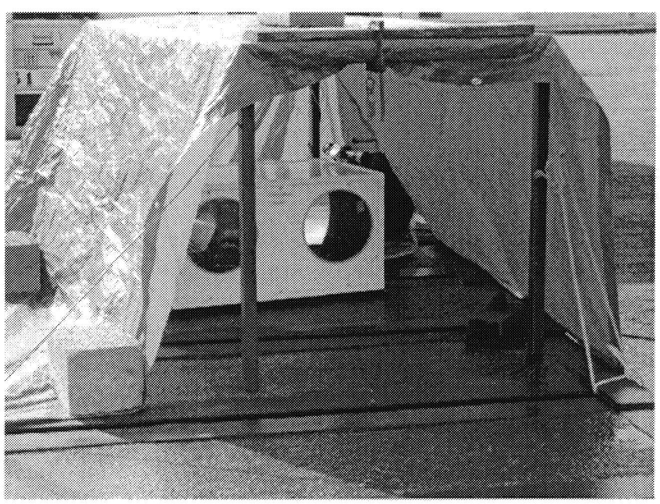

Figure 5. Set-up of the MSRT double source at the WTD 71 (near beginning of pier) location in an improvised shelter

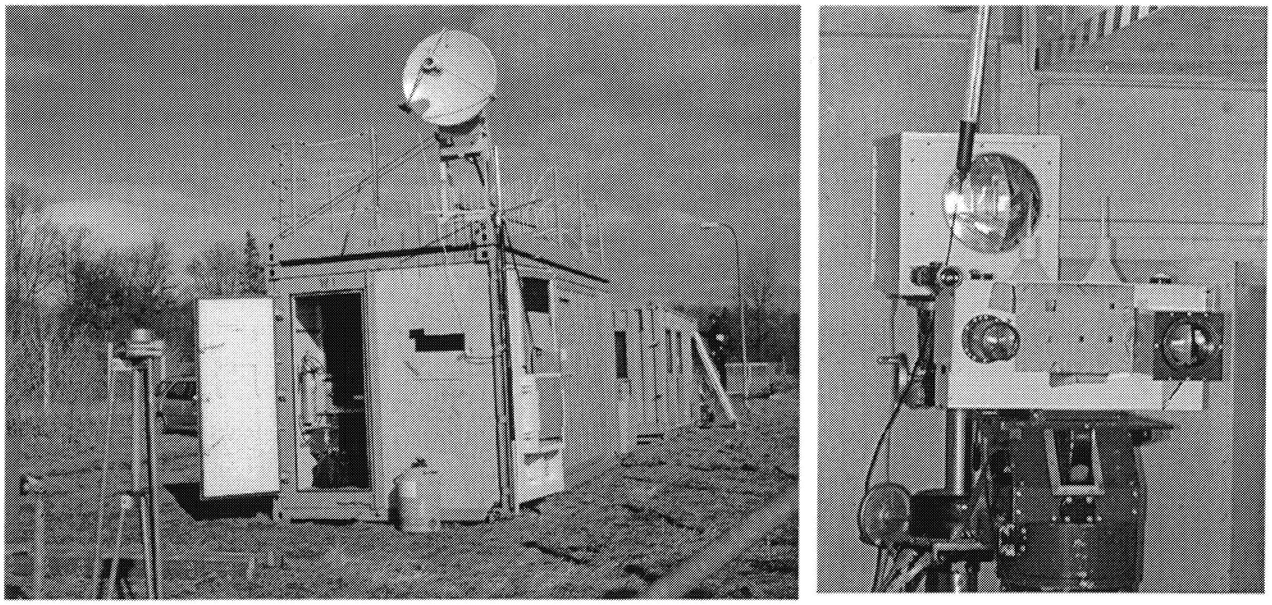

Figure 6. Container at Booknis Eck with radar transmitter on top (left) and MSRT receiver inside (right)

5. GENERAL WEATHER DATA

A series of weather plots is presented in Figure 7. The data in the upper plot show the air and sea temperature at 5.15 m. height at the buoy. The plots show the variability of the weather during the campaign: negative ASTD during the first days and some positive ASTD events later in the period. It was found that the temperatures at the various levels were fairly close during most of the trials period (within 0.5 °C). Only the sensor at the lowest height met problems during the high sea state on the 2nd of April, when it became wet. It is noted however, that even very small gradients (0.01 °/m) in the vertical temperature distribution may lead to important refraction effects. It is interesting to compare the temperature recordings at the three locations (buoy and shore stations). It appears that they follow precisely the same trend, although in daytime the air temperature at the shores becomes about one degree higher. The water temperature increases about one degree from the beginning to the end of the trials period. The relative humidity is rather high during part of the trial (from the 28th of March to the 2nd of April), which corresponds to the frequently poor visibility conditions in that period during the night and early morning.

The wind speed was generally quite high for this time of the year (6-10 m/s), while the wind direction started from North until the 31st of March, went to East until the 3rd and then to South, bringing warmer air. Consequently, apart from the evening of the 29th, the sea was rather rough during most of the time. The plots of the Solar Irradiance show that most of the time the skies were rather clear in daytime with partly clouds on the last five days in March. Occasional showers occurred on some of these days during short periods such as on the 25th around 12.00 and the 28th in the evening. Also some rain appeared on the 3rd of April. Most of the showers occurred locally and were of short duration. In the bottom plot of Figure 7 part of the output of from the Nephelometer is shown (Model 3563 from TSI). With this sophisticated sensor the scattering coefficient of the aerosol particles, sucked into the measurement volume is measured. This scattering coefficient and the absorption coefficient provide the total extinction coefficient, used in transmission calculations for aerosols. As well the backscatter as the integrated scatter are measured. The scattering is measured for three spectral filters, corresponding with the standard Red, Green and Blue filters from the color television application. The plot in Figure 7 is that of the blue channel (450 nm); the other channels were very similar in shape and magnitude. The data show a typical increase in scattering coefficient during the night, corresponding to the increase of the relative humidity. One has to realize that the Nehelometer was located at the pier and that part of the particles may have been produced by the breaking waves against the poles of the pier.

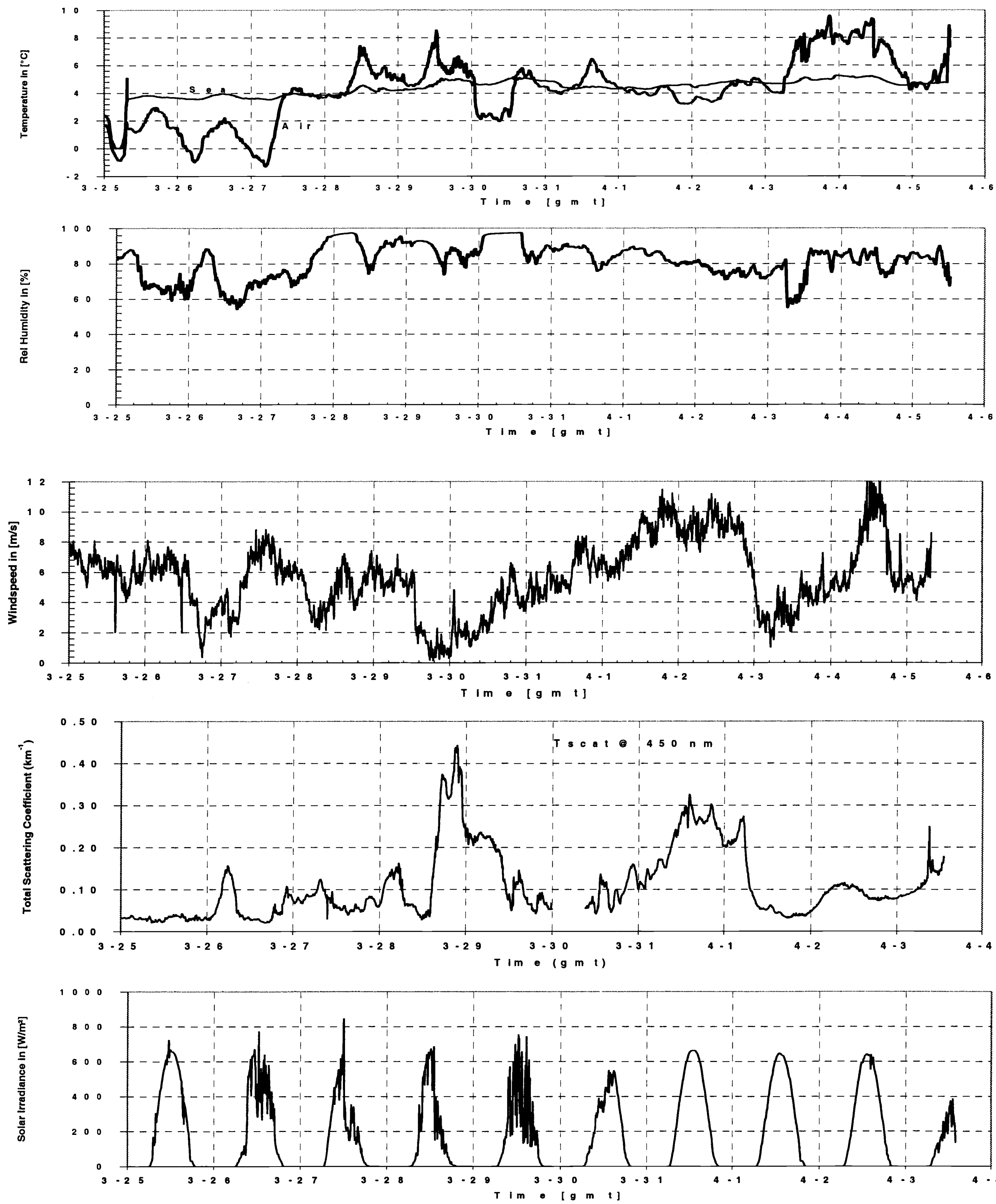

Figure 7. General weather data for the VAMPIRA trails; from top to bottom: Air and Sea temperature at mid-path buoy (5 m height); Relative Humidity at mid-path buoy (5m); Windspeed at Sürendorf; Scattering Coefficient (@ 450 nm) from Nephelometer at Sürendorf; Solar Irradiance at Booknis Eck

6. MULTI-BAND TRANSMISSOMETER AND PMS DATA

In this section data are presented, collected with the 7-band transmissometer. Figure 8 shows the data, measured with the 0.6, 1.5 and 4 μm channels as typical examples. The plot from the 0.6 μm channel shows that the visibility was poor during at least four periods, mostly at nighttime, when the transmission went down to zero. The 1.5 μm plot shows that for this waveband the transmission stays higher in foggy conditions, while the 4 μm channel is only affected by dense fog. The 4 μm channel shows gaps during some of the nights, when the Liquid Nitrogen was evaporated and the detector no longer cooled. Other artifacts in the plots are caused by LOS interruptions by ships and people. Most of them have been removed. Although the data have been averaged over one minute, the signal levels fluctuate considerably during some of the periods, much more than the noise level allows. These low frequency fluctuations are probably caused by atmospheric turbulence and surface waves at sea. Figure 9 shows close-ups of parts of the plots during periods of changing visibility for more channels simultaneously. For each of the data sets Log T(λ_1) - Log T(λ_2) plots have been produced. The different slopes show great similarity with those from Figure 3, predicted with the MODTRAN model. Apparently the particle size distribution was not the same for each of the selected periods. Striking is the fact that the transmission exceeds the 100% level during considerable parts of the time. This will further be discussed in section 7.

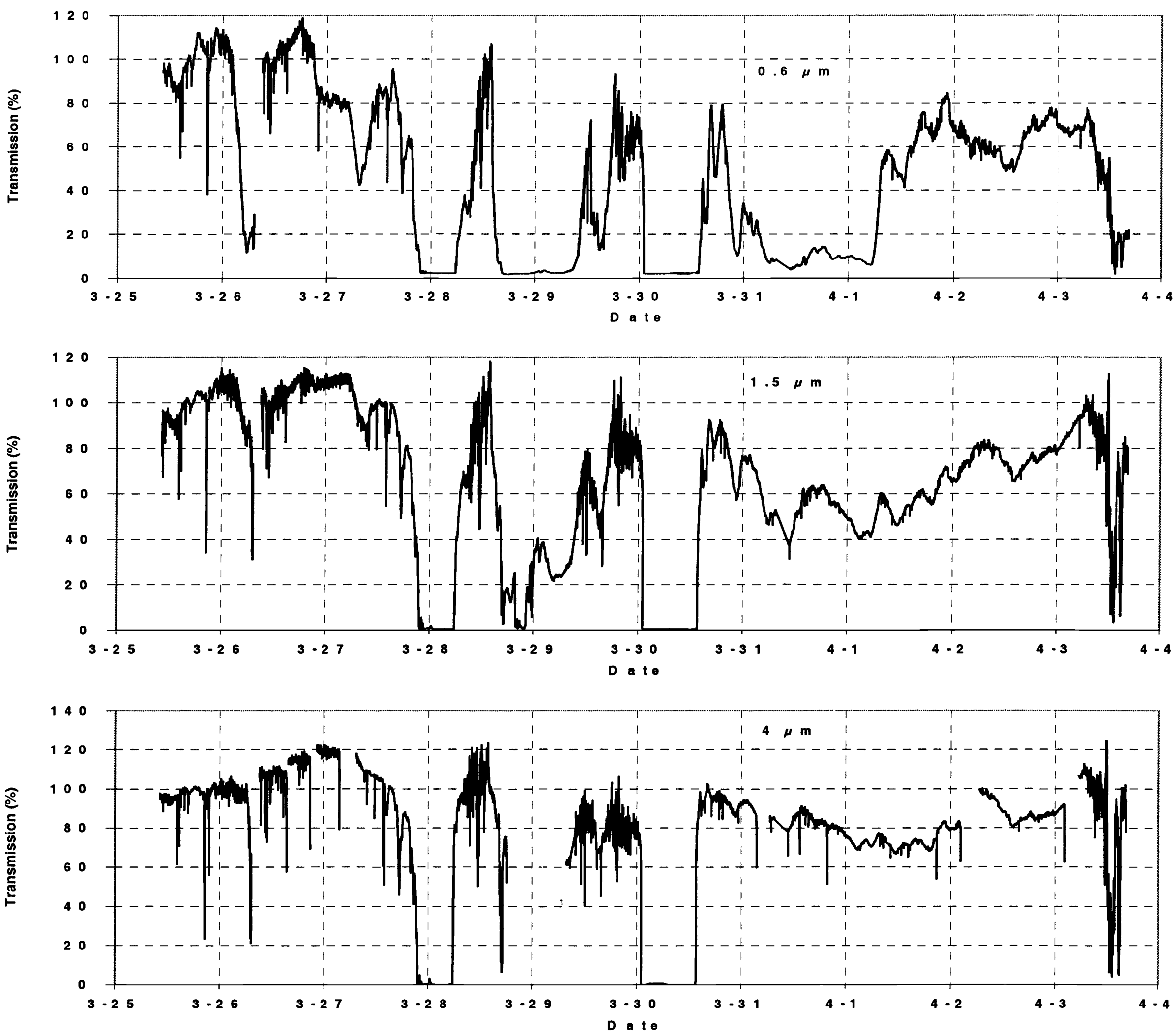

Figure 8. Transmission plots during the VAMPIRA trials for 3 of the 7 channels during the whole measurement period

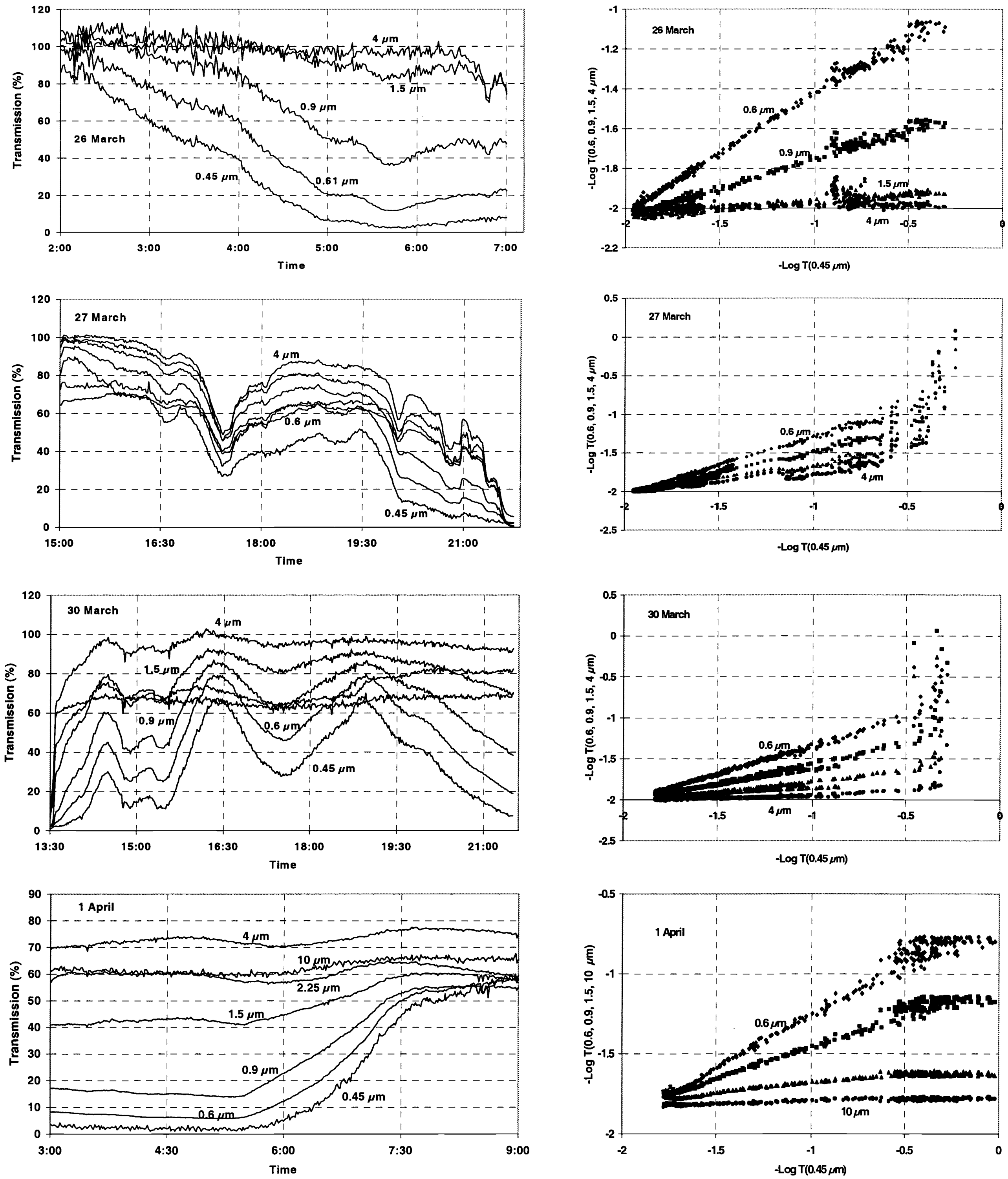

Figure 9. Detailed transmission plots accompanied with Log T(λ_1) - Log T(λ_2) plots for four periods during VAMPIRA.

Figure 10 shows sample results of the two PMS probes, taken in the center of the periods on 26 and 27 March, for which the transmission data are shown in Figure 9. The two plots show clearly the difference in the particle size distributions, resulting in differences in extinction coefficients for different wavelengths. The reason for the difference in the distribution is unclear as the wind-speed and direction were about the same. The plots of the extinction coefficients versus time for the same periods are shown in Figure 11. The extinction coefficients concern the extinction just caused by the aerosols (scattering + absorption), as calculated with the Mie scattering algorithms, applied at the same spectral bands as those of the MSRT. The time plots show a similar behavior as that, measured with the transmissometer plots in Figure 9 and with the Nephelometer plot, shown in Figure 7. This indicates that the fog came up rather homogeneous along the path. The plots of the extinction coefficients for four bands versus 0.45 μm are very similar to the Log T(λ_1) - Log T(λ_2) plots in Figure 9 and show the same differences for the two selected periods. This illustrates, that the data, obtained with the transmissometer, the Nephelometer and the PMS probes correspond quite well.

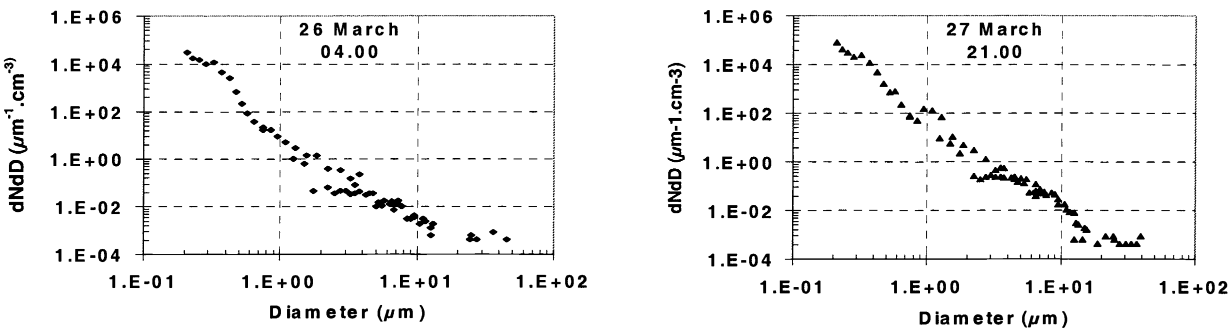

Figure 10. Samples results of particle size distribution measurements, taken with the PMS probes at the Sürendorf pier.

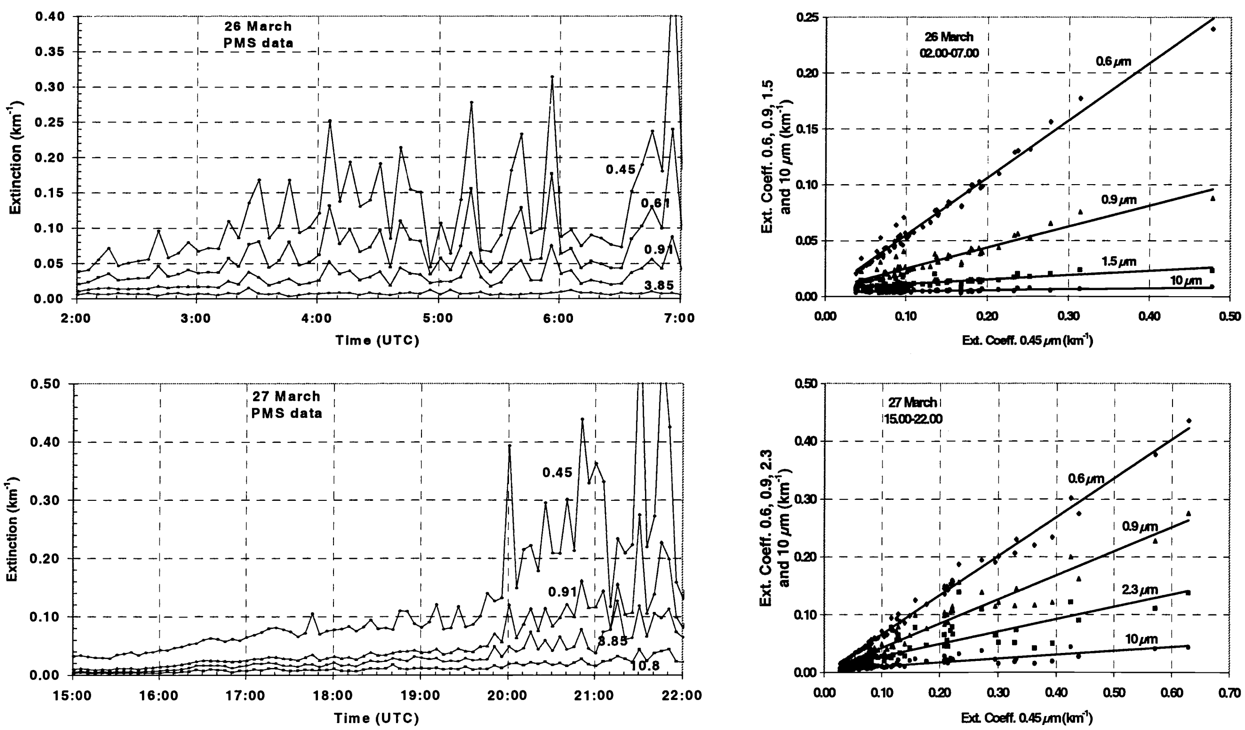

Figure 11. Plots of the extinction coefficients by scattering at four wavelengths versus time and Ext-Ext plots for the selected periods on 26 and 27 March, obtained with the PMS probes at the pier

7. DISCUSSION

The transmission measurements over the Eckernförde Bucht during the VAMPIRA trials show some interesting results. Transmission levels above 100% appear due to the relative short range (8.6 km) and large height of source and receiver (about 8 m). The consequence is that reflections at the water surface may enter the large FOV 's of the receivers (>1°). For longer atmospheric paths and lower heights of source and receiver, the light beams skim the water surface so that they are refracted into the sky most of the time in the boundary layer before they reflect [6]. During VAMPIRA the direct beams stay about 6 m above the water surface. The beam of the sources has a total height of 20 m at the center of the path, which is more than enough to create a mirror image on the sea surface. For a perfectly flat sea surface this means that the expected transmission values have to be doubled. The two light sources (the real and the reflected) will not interfere because of their size and short range. In reality the sea surface is not flat and a number of small reflection centers at the wave tops will appear. The sum of all this small reflections may however be larger than the intensity from the single source. The maximum measured transmission values in all channels are between 110 and 120%, which is about a factor 1.5-2.0 (for 0.45 μm: 3) times the predicted value, corresponding to the statement before. The factor 2 exceeds by far the measurement error of the transmissometer.

In addition to the surface reflections forward scattering by aerosols may contribute to increased transmission values, especially for lower visibility and rainy conditions. In the total extinction coefficient of aerosols it is assumed that all scattered radiation is lost outside the LOS and sensor pupil. Due to the large FOV of the receivers however they tend to collect a considerable amount of the radiation, scattered in forward direction. Realizing that the beam width is spread to about 140x40 (HxV) m over the path of 8.6 km, it is clear that especially the visual/near IR channels with FOV's of more than 70 mrad may collect spurious radiation. Zeisse [19] estimates that for his narrow band system the contribution by forward scattering is about a few percent maximum. In our case a similar consideration leads to a forward scattering contribution of up to 50%. This estimation is of course strongly dependent on the geometry (homogeneity of the particle concentration along the path) and the phase function of the particles. A more detailed analysis of the effect is beyond the scope of this paper.

The next analysis concerns the multi-band transmission data for periods with changing visibility conditions. As Figure 9 shows, the ratio of the extinction coefficients in different spectral bands remains nearly the same when the visibility changes. This is an indication that the particle size distribution does not change but only the concentration, which was also predicted by the NAM and Rural models (Figure 3). In order to compare the slopes of the Log $T(\lambda_1)$ – Log $T(\lambda_2)$ plots for the different days and spectral band combinations, Table 2 has been prepared. The data show a decrease of the slope ratios for the combinations of the longer wavebands with the shortest band (0.45 μm). The ratios become the smallest for the 26th of March and the 1st of April, when the smaller particles were relatively more represented than the bigger particles. Apparently the fog was more of a Rural or Urban nature. The fog of 27 March was apparently more of a maritime nature (bigger in size), while on the 30th of March the character of the fog was somewhat in between.

Table 2. Slopes of Log $T(\lambda_1)$ – Log $T(\lambda_2)$ and Ext. (λ_1) - Ext. (λ_2) plots for different data sets and aerosol models

Day/Model	0.61/0.45	0.91/0.45	1.53/0.45	2.25/0.45	3.85/0.45	10.8/0.45	1.53/0.61	3.85/0.91
26-03	0.585	0.294	0.077	0.045	0.019	0.031	0.132	0.066
27-03	0.740	0.594	0.418	0.276	0.344	0.283	0.565	0.579
30-03	0.715	0.488	0.236	0.063	0.076	0.006	0.330	0.156
01-04	0.645	0.391	0.113	0.030	0.025	0.031	0.175	0.064
26-03 PMS	0.513	0.188	0.039	0.008	0.001	0.008	0.076	0.005
27-03 PMS	0.677	0.418	0.268	0.215	0.193	0.067	0.396	0.462
NAM	0.613	0.641	0.543	0.688	0.335	0.150	0.867	0.489
Rural	0.445	0.304	0.142	0.155	0.097	0.078	0.307	0.259

The data in Table 2 and the plots in Figures 9 and 11show, that the atmosphere (haze and fog) during the VAMPIRA trials was rather homogeneous. No local effects, such as shown in Figure 1 were found. The transmission values obtained via the extinction data from the PMS probes, correspond quite well with those, directly measured with the MSRT system after subtraction of the molecular extinction and surface reflection effects. The slopes of the Log $T(\lambda_1)$ – Log $T(\lambda_2)$ plots are generally somewhat smaller for the data obtained with the PMS probes.

ACKNOWLEDGEMENTS

The personnel of the German site WTD 71 and in particular Mr. Wehr is greatly acknowledged for the support, given during the VAMPIRA trials. The German Ministry of Defense and in particular people from FGAN are greatly acknowledged for the sponsoring and the organization of the trials. Peter Fritz from TNO-FEL is acknowledged for his support in the set-up of the meteorological stations at both sides and during the installation of the meteo buoy. The work, described in this paper was partly sponsored by the Royal Netherlands Navy and the US Office of Naval Research.

REFERENCES

[1] The IR&EO Systems Handbook, Vol.5, *IR Search and Track Systems*, SPIE Opt. Eng. Press, 1993
[2] The Infrared & Electro-Optical Systems Handbook, Vol.2, *Atmospheric Transmission*, SPIE Opt. Eng. Press, 1993
[3] F.X. Kneizys, L.W. Abreu, G.P. Anderson et al, *The MODTRAN 2/3 Report and LOWTRAN 7 Model*, prepared by Ontar Corporation, North Andover (MA)
[4] Douglas R. Jensen et al, *Electro-Optical propagation assessment in coastal environments (EOPACE): summary and accomplishments*, Opt. Eng. 40(8), (August 2001)
[5] Arie N. de Jong et al, *TG16 point target detection experiment POLLEX, Livorno 2001*, SPIE Volume 4820, Infrared Technology and Applications XXVIII, Seattle, July 2002
[6] Arie N. de Jong, *Refraction effects of atmospheric inhomogeneities along the path*, SPIE Volume 5237, Barcelona, September 2003
[7] Arie N. de Jong et al, *Atmospheric refraction effects on optical/IR sensor performance in a littoral-maritime environment*, submitted for publication in Applied Optics March 2004
[8] Arie N. de Jong et al, *Scintillation measurements during the EOPACE November '96 and August '97 campaigns*, SPIE Volume 3433, Propagation and Imaging through the Atmosphere II, San Diego, July 1998
[9] Arie N. de Jong, *Intensity variations of small airborne incoming targets, popping-up above the horizon*, SPIE Vol. 5237, Barcelona, September 2003
[10] J. Luc Forand et al, *An extensive analysis of Low-Level IR transmission measurements taken over a 15 km path during EOPACE with IRBLEM*, SPIE Vol. 3433, San Diego, July 1998
[11] Arie N. de Jong et al, *Report on Smoke Week IX, held from 4-22 May 1987 at Eglin Air Force Base, Florida*, TNO Report FEL 1987-100
[12] Arie N. de Jong et al, *Results of IR experiments during Duck-EOPACE, February/March 1999*, TNO report FEL-99-A182, September 1999
[13] Stuart G. Gathman et al, *Electro-optical propagation just above wave tops as predicted by ANAM, the Advanced Navy Aerosol Model*, Proceedings NATO-SET Symposium TP/2, Naples (It.), March 1998
[14] Dan L. Hutt et al, *Comparison of marine aerosol model predictions with extinction and size distribution measurements*, SPIE Vol. 3125, San Diego, July 1997
[15] Filip P. Neele et al, *Aerosol production in the surf zone and effects on IR extinction*, Proceedings NATO-SET Symposium TP/2, Naples (It.), March 1998
[16] Stephen M Doss-Hammel et al, *Low-altitude infrared propagation in a coastal zone: refraction and scattereing*, Applied Optics, Vol. 41, No. 18, June 2002
[17] Alexander M.J. van Eijk et al, *Near-surface aerosol transmission in the marine environment*, SPIE Vol. 4884, Crete, September 2002
[18] Arie N. de Jong et al, *Description of a 7-channel MSRT system: Multi Spectral Radiometer Transmissometer*, TNO report FEL-99-I028, February 1999
[19] Carl R. Zeisse et al, *Measurement of low-altitude infrared propagation*, Applied Optics, Vol.39, No. 6, Febr. 2000